Lecture 7:

Evidence of evolution:
Direct observations

Course 410

Molecular Evolution

Antibiotic resistance-bacteria

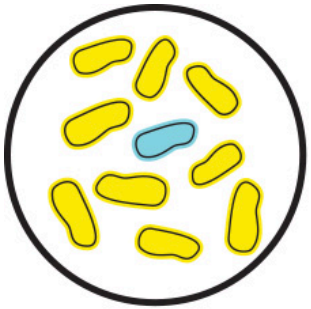

Our body is **home to countless microbes**. Some may be resistant to antibiotics

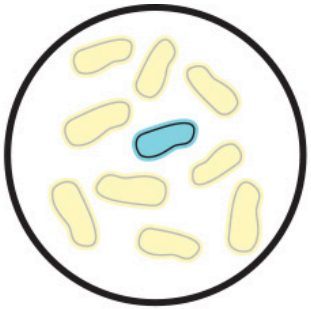

Antibiotics kill the bacteria causing the infections as well as the good bacteria

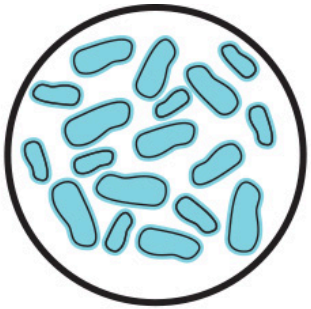

The antibiotic-**resistant bacteria** are now able to **grow and take over**

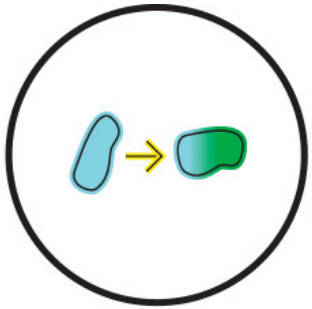

Some bacteria may **give** their antibiotic **resistance to other bacteria**

Normal bacterium **Resistant bacterium** **Dead bacterium**

Targeting Antibiotic Resistance

*Mathieu F. Chellat, Luka Raguž, and Rainer Riedl**

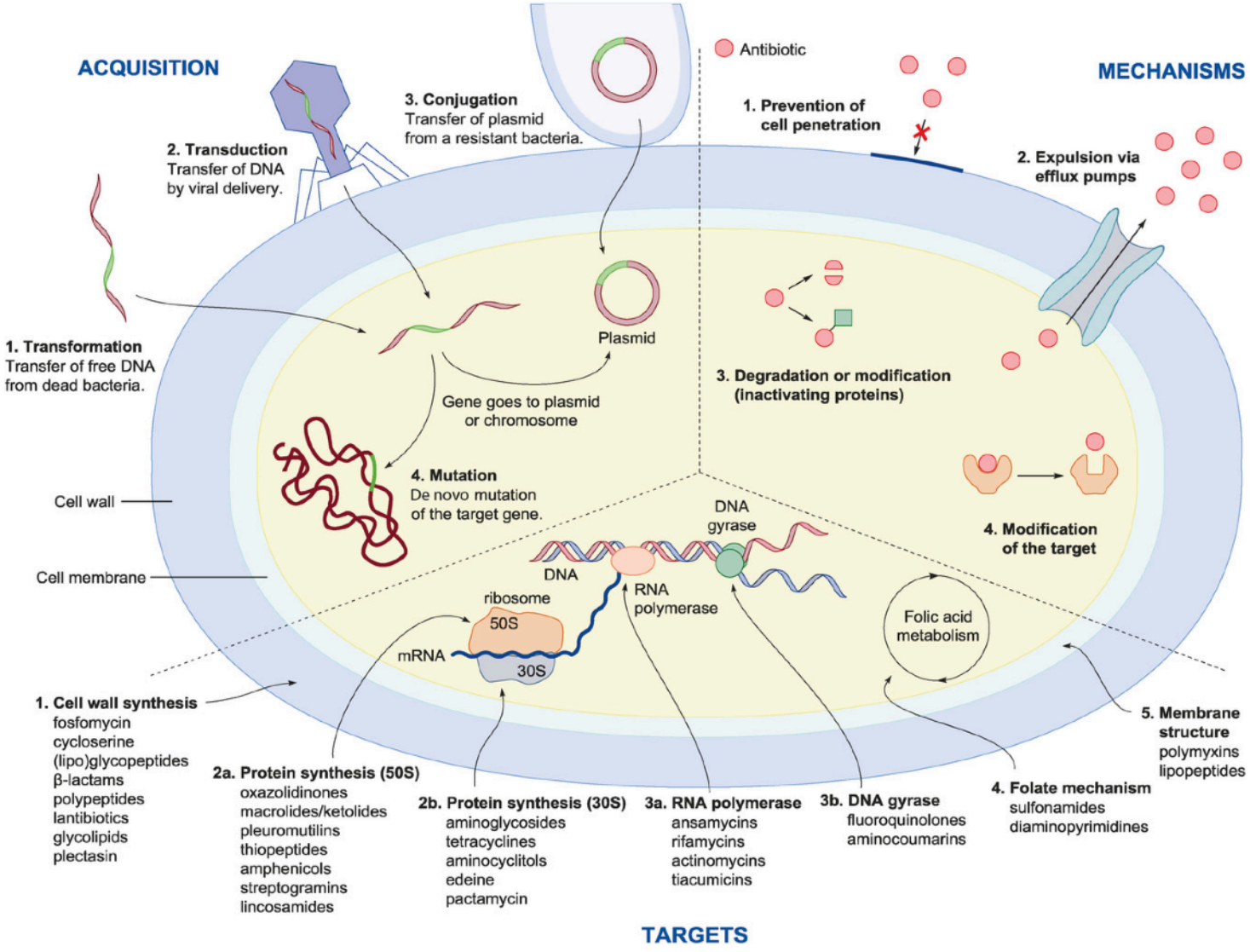

nature microbiology

Article

https://doi.org/10.1038/s41564-023-01472-1

Genomic epidemiology reveals multidrug resistant plasmid spread between *Vibrio cholerae* lineages in Yemen

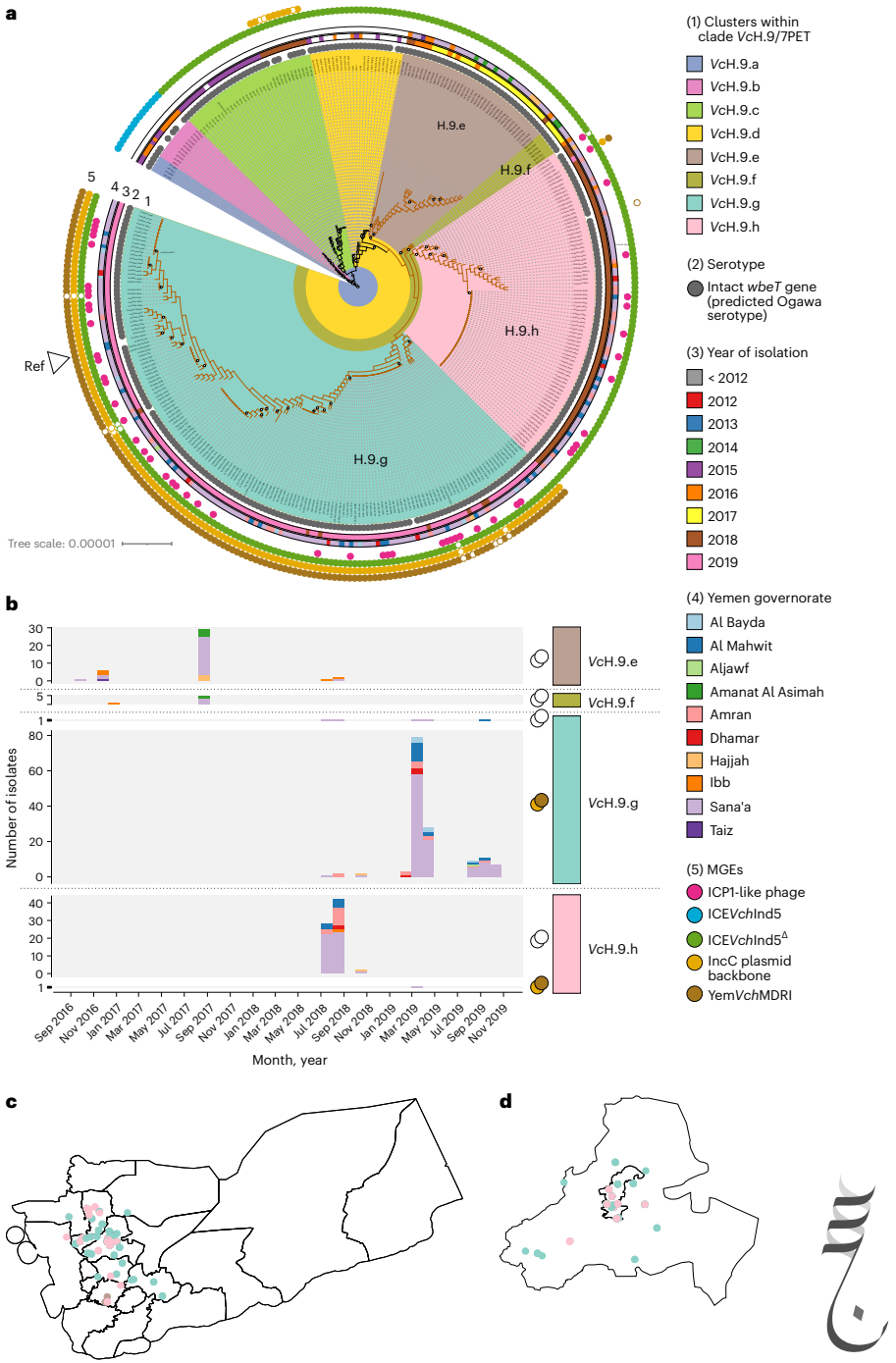

Fig. 2 | Phylogenetic diversity and spatio-temporal distribution of *V. cholerae* 7PET-T13 isolates (*Vc*H.9) from Yemen. a, Subtree of the ML phylogeny of 456 7PET genomes mapped to reference *Vc*H.9 strain CNRVC190243 genome, including 335/456 genomes covering *Vc*H.9 (as defined in Supplementary Fig. 5), which corresponds to the 7PET-T13 sub-lineage and close South Asian relatives. The full tree containing the 456 genomes is available as supplementary material on figshare (https://doi.org/10.6084/m9.figshare.16595999) and was obtained based on 2,092 SNP sites from concatenated whole-chromosome alignments. Brown branches indicate the clade grouping all Yemeni 7PET-T13 isolates. Bootstrap support greater than 70% is indicated by white circles. Phylogenetic clusters within *Vc*H.9 are highlighted with background colours (legend key 1). Coded tracks outside the tree depict the serotype of isolates (ring 2) as predicted from genomic data, year of isolation when isolated in 2012 or later (ring 3) and the governorate of isolation if in Yemen (ring 4). The presence of MGEs is indicated by coloured circles in the outermost track (ring 5): ICP1-like phage (pink), SXT ICE ICE*Vch*Ind5 (blue), ICE*Vch*Ind5$^{\Delta}$ that is featuring the characteristic 10-kb deletion in the variable region III (green), IncC plasmid backbone (light brown) and the MDR PCT Yem*Vch*MDRI (dark brown); filled and unfilled circles indicate different levels of coverage in assemblies (as in Fig. 1 legend). The position of the reference sequence to which all other genomes were mapped to generate the alignment is labelled. The scale bar represents the number of nucleotide substitutions per site. **b**, Frequency of each phylogenetic subcluster among Yemen isolates per month since the onset of the Yemen outbreak. Where relevant, the cluster group is subdivided by the presence or absence of the IncC plasmid as indicated by the filled brown (present) or open (absence) circle on the right of the chart. The contribution of each governorate of isolation is indicated by the coloured portion of each bar. **c**,**d**, A map of Yemen governorates (**c**) and a focus on the Sana'a and Amanat Al Asimah governorates (inner and outer capital city; **d**), with dots corresponding to isolates, coloured by phylogenetic subcluster.

Pesticide resistance-arthropods

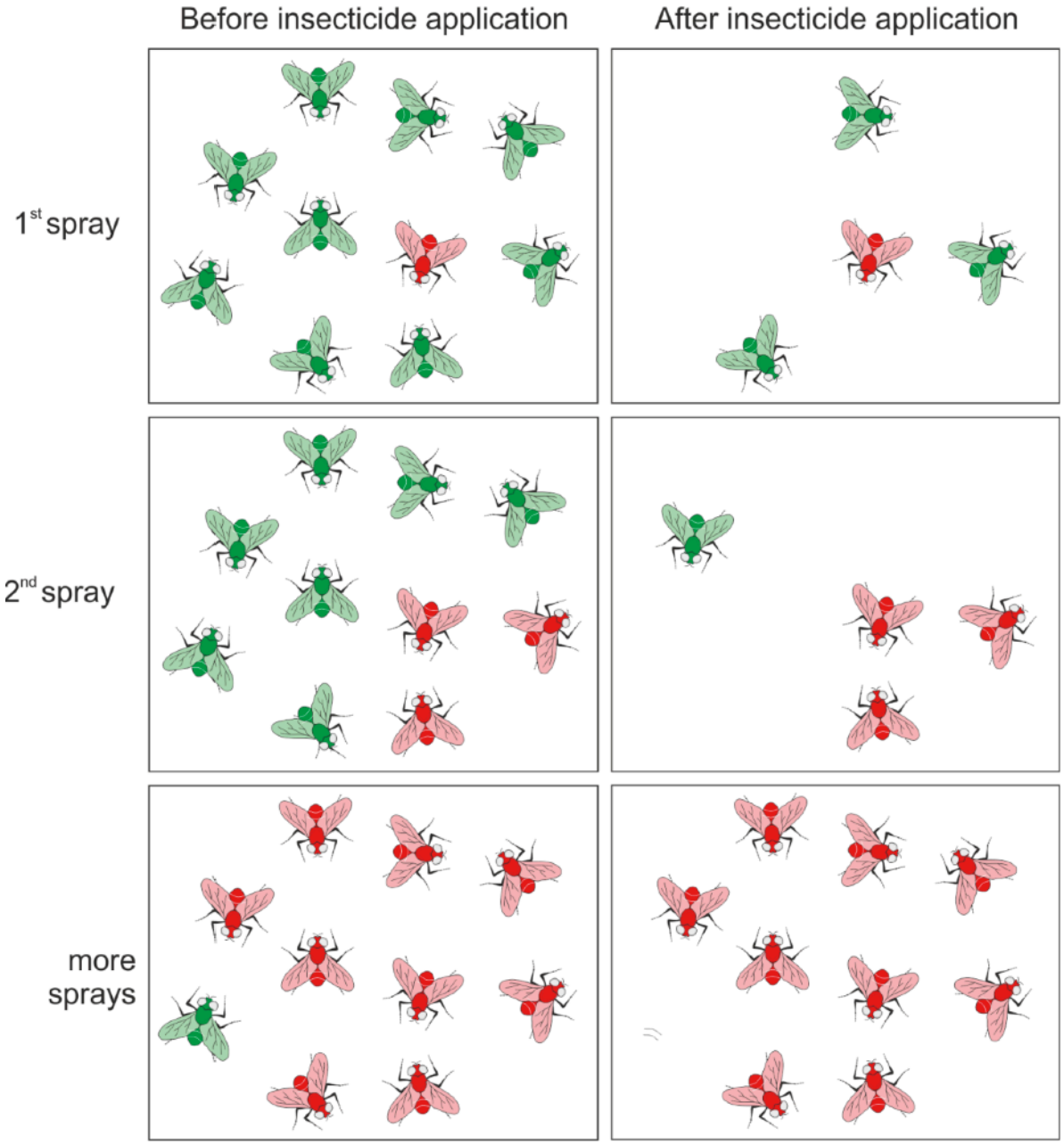
Before insecticide application
After insecticide application
1st spray
2nd spray
more sprays

ECOLOGY LETTERS WILEY

Pesticide resistance in arthropods: Ecology matters too

Audrey Bras[1,2] | Amit Roy[2] | David G. Heckel[3] | Peter Anderson[1] | Kristina Karlsson Green[1]

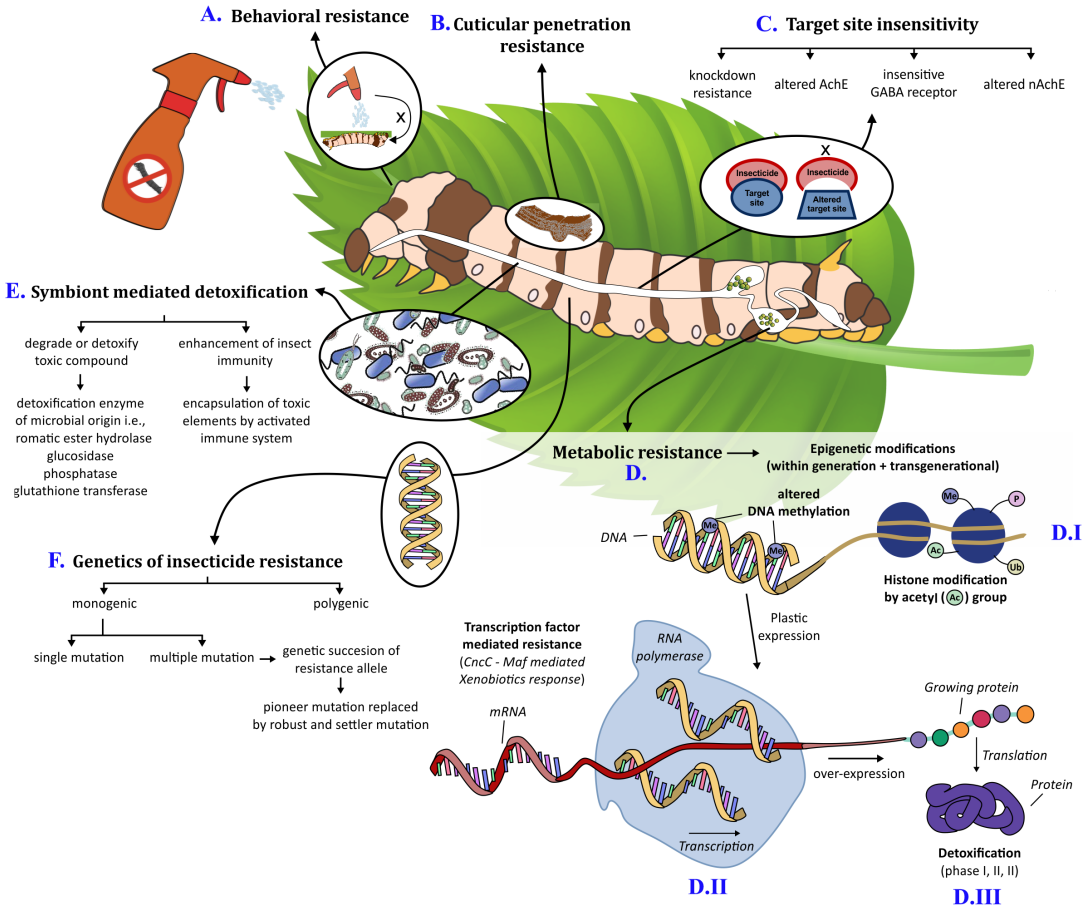

FIGURE 1 Mechanisms for pesticide resistance evolution in the insect. (A) Resistance acquisition via avoidance of the toxin, that is insecticides often fail to reach target insects under the leaf. (B) Reduce toxin penetrability through thickening of the insect cuticle. (C) Mutation in the binding site inside the target pest causes pesticide insensitivity. (D) Pesticide metabolism exploiting internal molecular machinery. I modifications may occur at the epigenetic level via DNA methylation or histone modification, leading to target gene expression alteration upon pesticide exposure. Epimutations are often heritable. II transcription factors (TFs) can modulate the expression of xenobiotic response elements, that is CncC-Maf mediated xenobiotic response. III overexpression of phase I (i.e. Cyt P450s), phase II (i.e. GSTs), phase III (i.e. ABC transporters) enzymes can lead to detoxification or excretion of the entomotoxic pesticide molecules. (E) In-house microbial symbionts can facilitate resistance development via detoxifying the toxic compound or facilitating the encapsulation of toxic molecules by activating the insect's immune system. (F) Single gene or multigene mutations can facilitate genetic resistance against pesticides.

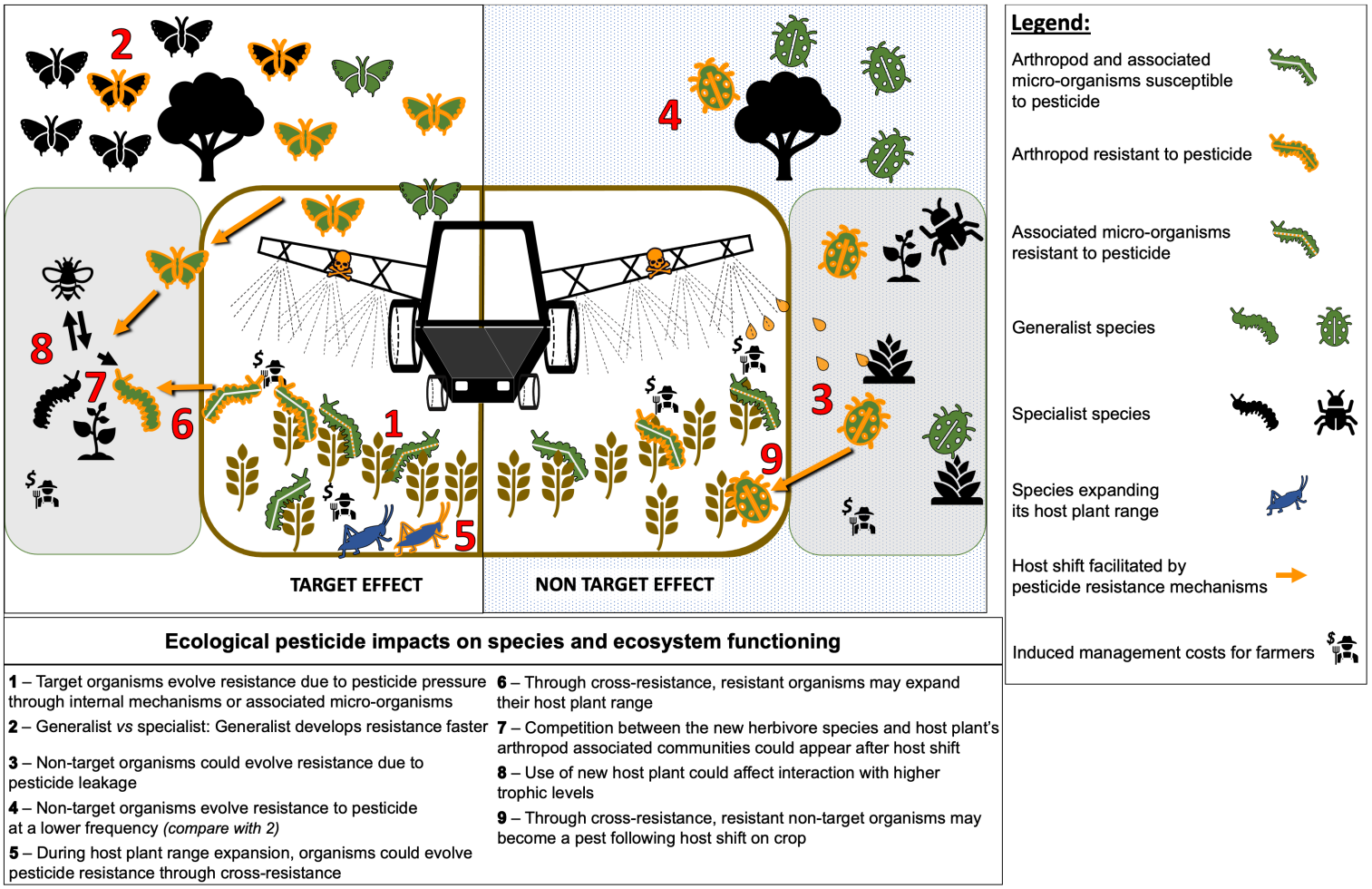

FIGURE 3 Scheme over pesticides' direct and indirect impacts on ecosystem functioning following cross-resistance, from target species to non-target species. Pesticides, the development of resistance due to their use and their potential side effects are represented in yellow. The impacts listed in the figure are not exhaustive.

HIV

HIV | ˌāCHˌīˈvē |

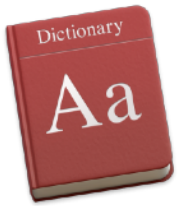

abbreviation

human immunodeficiency virus, a retrovirus which causes AIDS: *[as modifier] : HIV infection.*

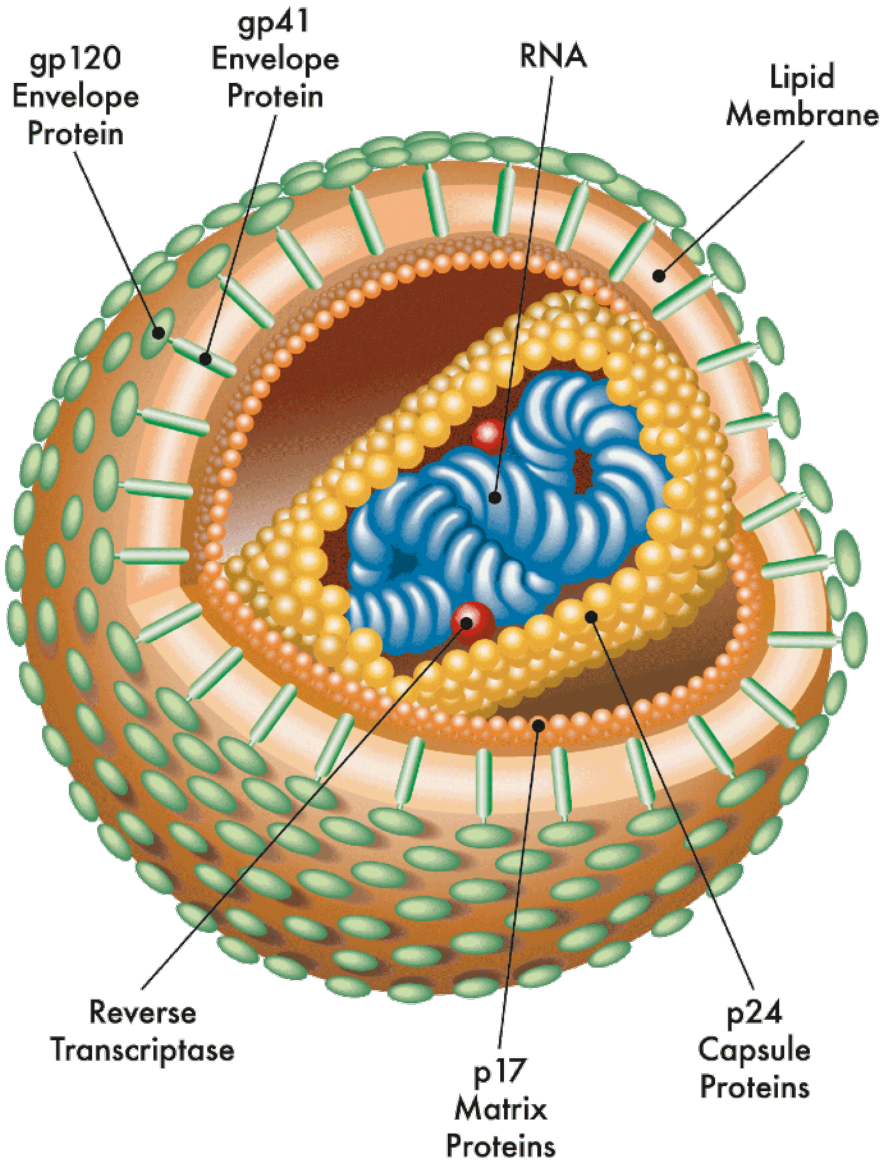
gp120
Envelope
Protein
gp41
Envelope
Protein
RNA
Lipid
Membrane
Reverse
Transcriptase
p17
Matrix
Proteins
p24
Capsule
Proteins

Types of Viruses

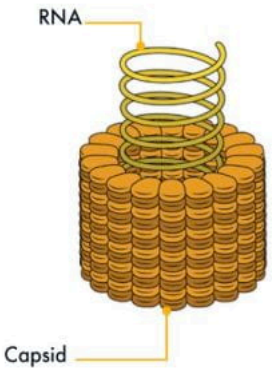

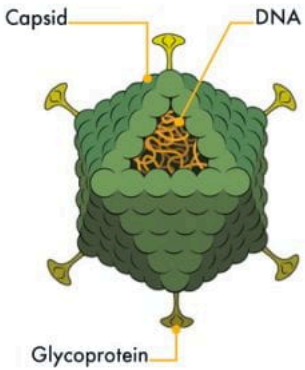

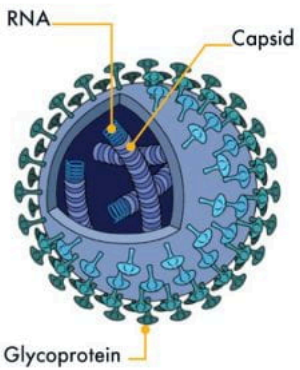

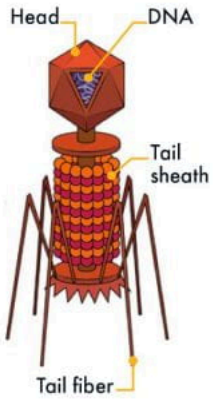

Helical viruses, like the Tobacco Mosaic Virus, which infects a number of different types of plants, have a slinky-shaped capsid that twists around and encloses its genetic material.

Polyhedral viruses, like adenoviruses, which are known to cause a range of illnesses from pink eye to pneumonia, are composed of genetic material surrounded by a many-sided capsid, usually with 20 triangular faces.

Spherical viruses, like the infamous Coronavirus, are essentially helical viruses enclosed in a membrane known as an envelope, which is spiked with sugary proteins that assist in sticking to and entering host cells.

Complex viruses, like bacteriophages, which infect and kill bacteria, resemble a lunar lander, and are composed of a polyhedral "head" and a helical body (or "tail sheath"), and legs (or "tail fibers") that attach to a cell membrane so that it can transfer its genetic material.

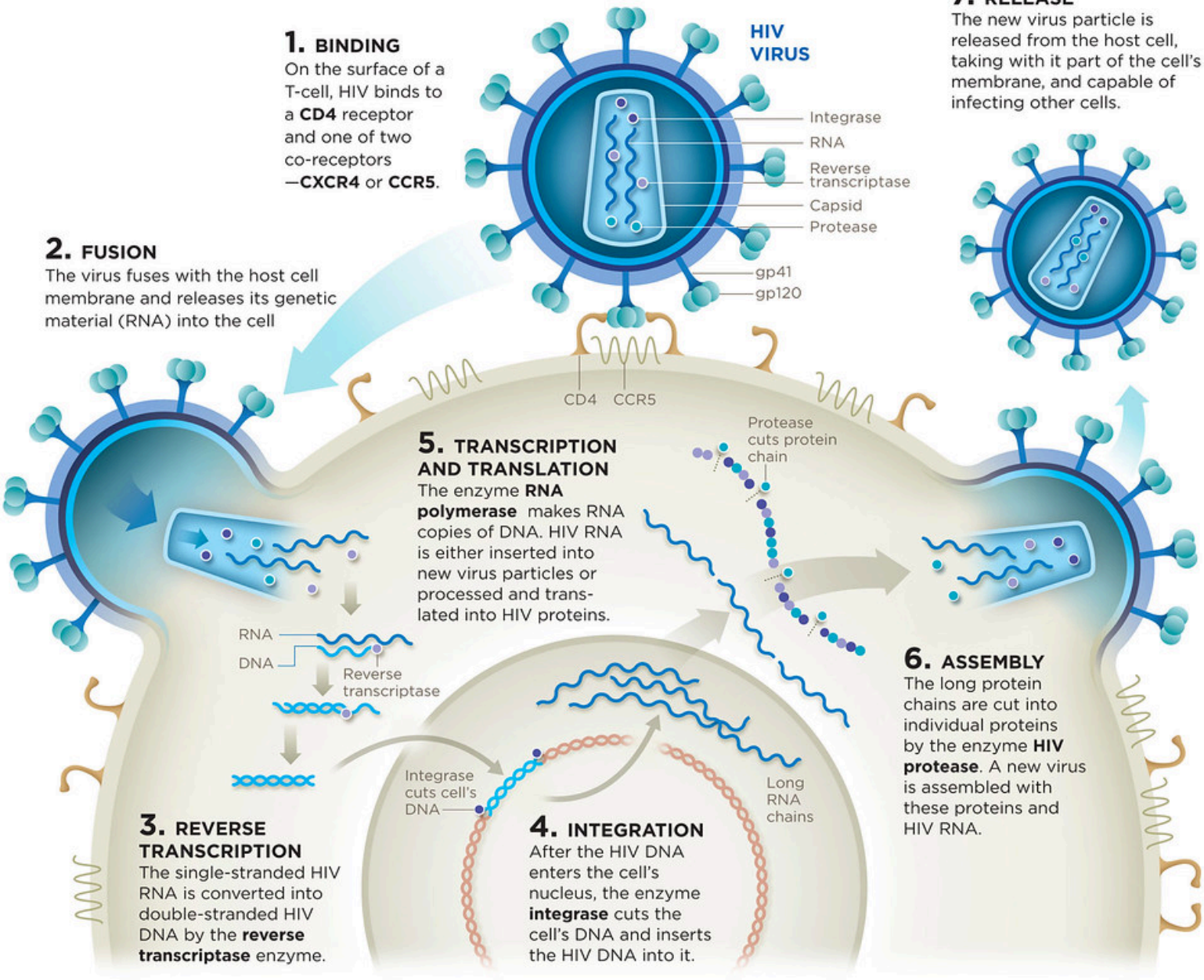
1. BINDING
On the surface of a T-cell, HIV binds to a CD4 receptor and one of two co-receptors —CXCR4 or CCR5.
HIV VIRUS
Integrase
RNA
Reverse transcriptase
Capsid
Protease
gp41
gp120
7. RELEASE
The new virus particle is released from the host cell, taking with it part of the cell's membrane, and capable of infecting other cells.
2. FUSION
The virus fuses with the host cell membrane and releases its genetic material (RNA) into the cell
CD4
CCR5
5. TRANSCRIPTION AND TRANSLATION
The enzyme RNA polymerase makes RNA copies of DNA. HIV RNA is either inserted into new virus particles or processed and translated into HIV proteins.
Protease cuts protein chain
RNA
DNA
Reverse transcriptase
6. ASSEMBLY
The long protein chains are cut into individual proteins by the enzyme HIV protease. A new virus is assembled with these proteins and HIV RNA.
Integrase cuts cell's DNA
Long RNA chains
3. REVERSE TRANSCRIPTION
The single-stranded HIV RNA is converted into double-stranded HIV DNA by the reverse transcriptase enzyme.
4. INTEGRATION
After the HIV DNA enters the cell's nucleus, the enzyme integrase cuts the cell's DNA and inserts the HIV DNA into it.

1 Treatment begins

2 Viral load falls as drug-sensitive HIV disappears

3 Drug-resistant HIV continues to grow despite the presence of treatment. Over time, growth of these viruses can cause viral load to rise again.

drug-sensitive HIV drug-resistant HIV

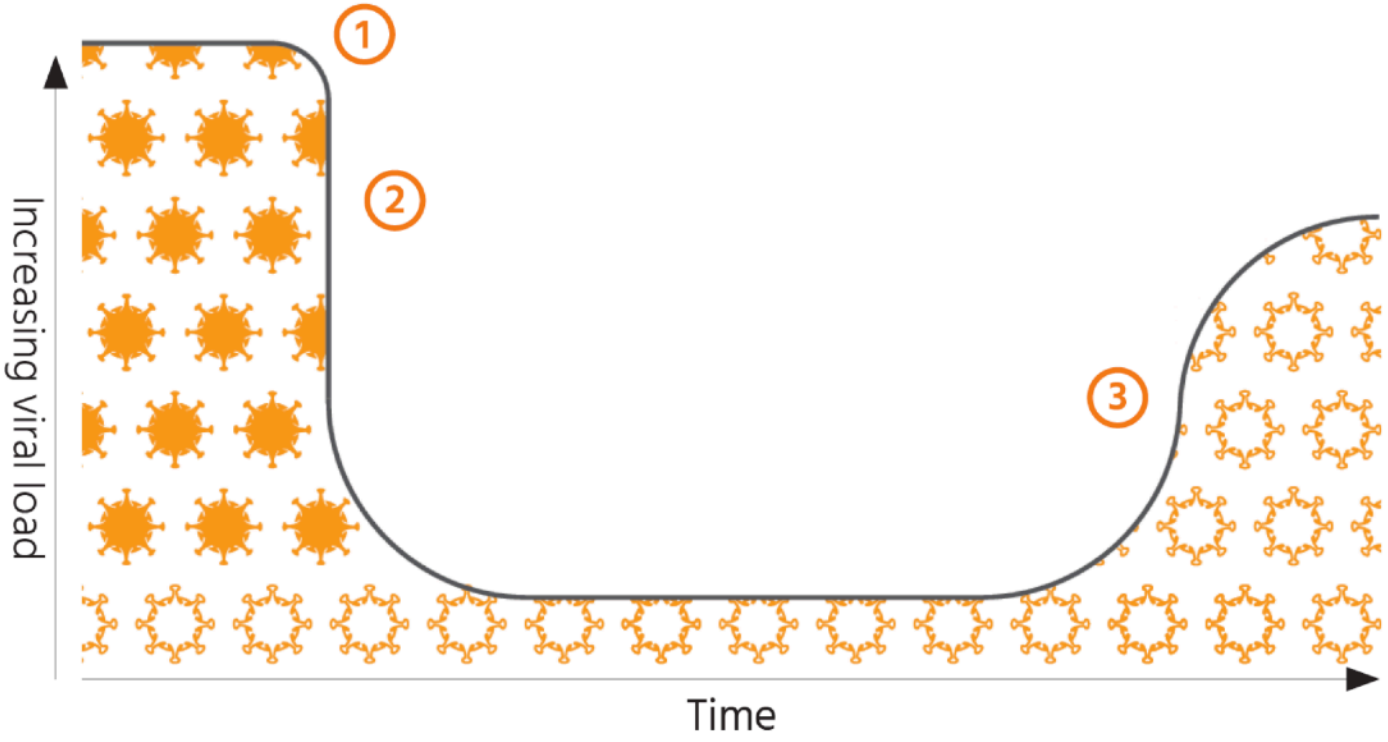

Share of the population infected with HIV, 2019

The share of people aged 15 to 49 years old who are infected with HIV.

Our World in Data

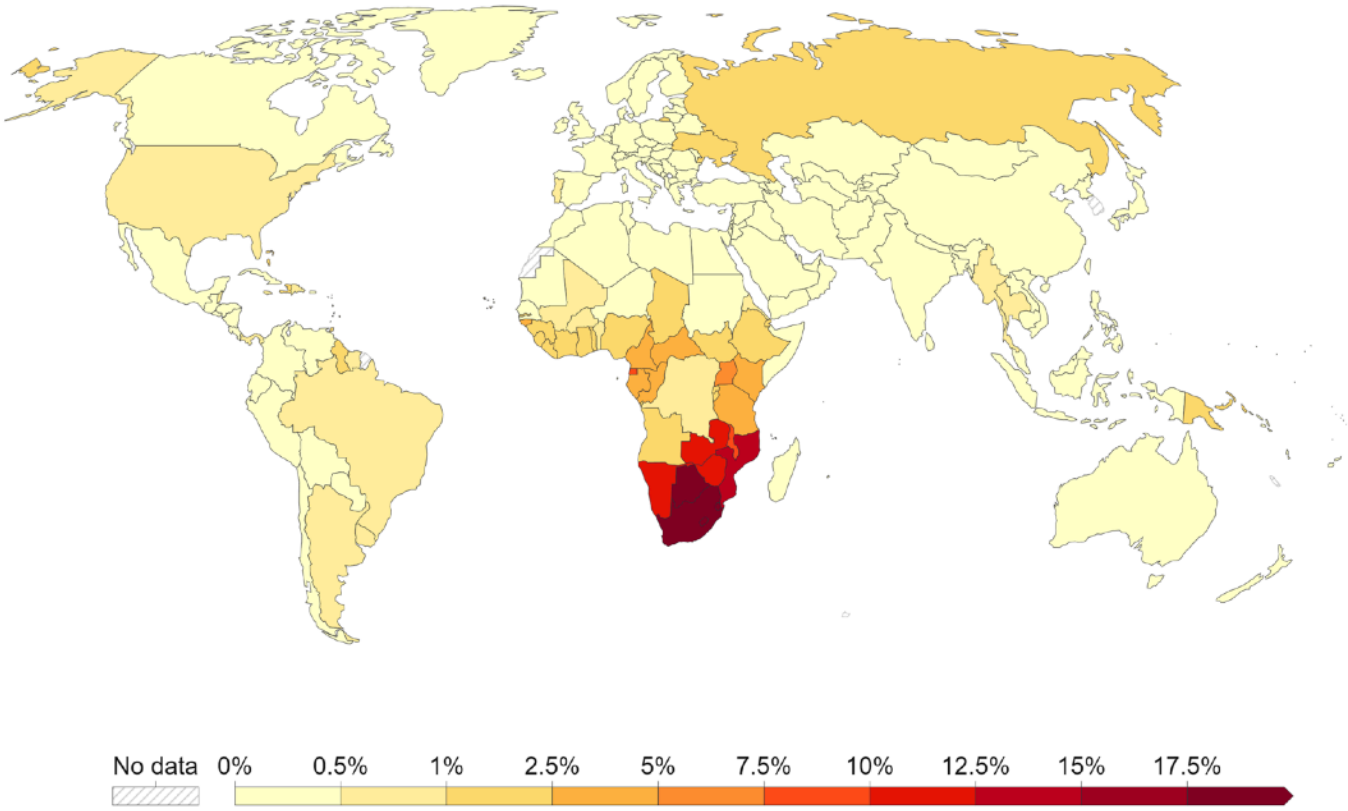

Source: IHME, Global Burden of Disease (2019)

OurWorldInData.org/hiv-aids • CC BY

Implementation of national HIV drug resistance surveys, 2004-2021

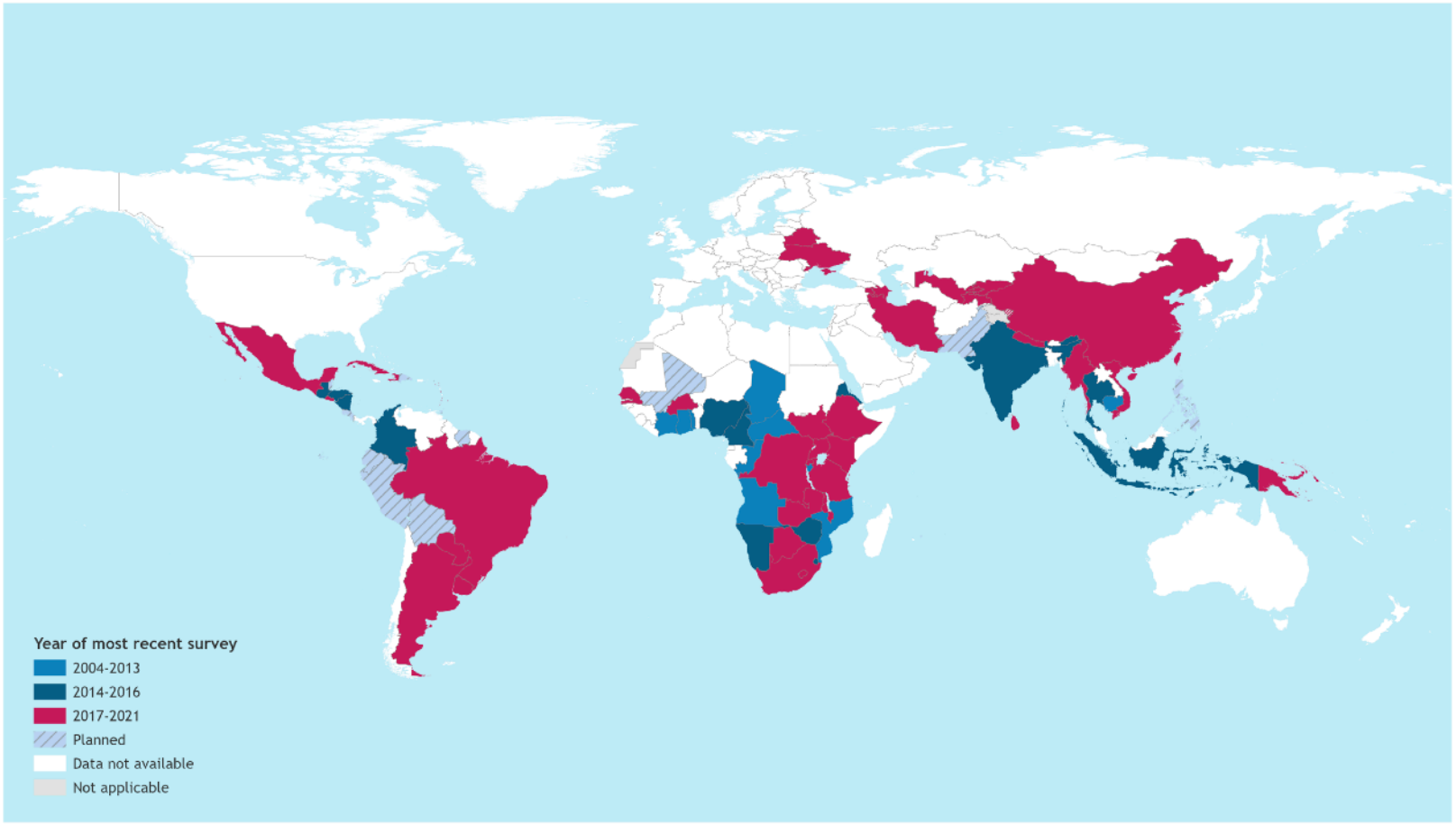

The designations employed and the presentation of the material in this publication do not imply the expression of any opinion whatsoever on the part of WHO concerning the legal status of any country, territory, city or area or of its authorities, or concerning the delimitation of its frontiers or boundaries. Dotted and dashed lines on maps represent approximate border lines for which there may not yet be full agreement.

Data Source: World Health Organization
Map Production: WHO GIS Centre for Health, DNA/DDI

Map Creation Date: **12 October 2021**

World Health Organization

Peppered moth

Biston betularia

Industrial Melanism, History of

DW Rudge, Western Michigan University, Kalamazoo, MI, USA

Figure 1 *Biston betularia*: one typical and one *carbonaria* resting on a lichen-covered tree in unpolluted country (Dorset); and, one typical and one *carbonaria* resting on blackened and lichen-free bark in an industrial area (the Birmingham district). These photos originally appeared separately as Plates 14 and 15 in Ford (1975).

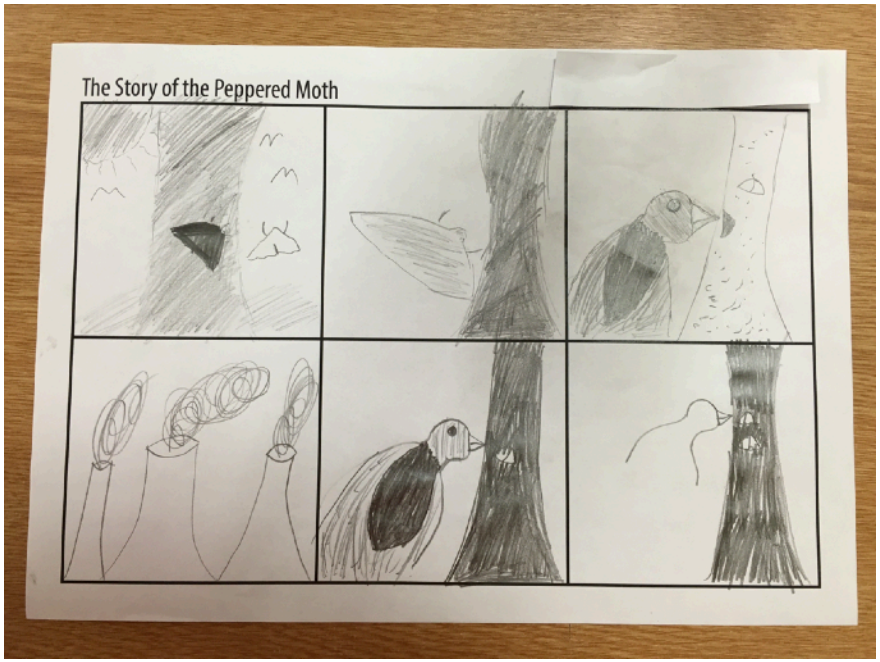

Pre-Industrial Revolution

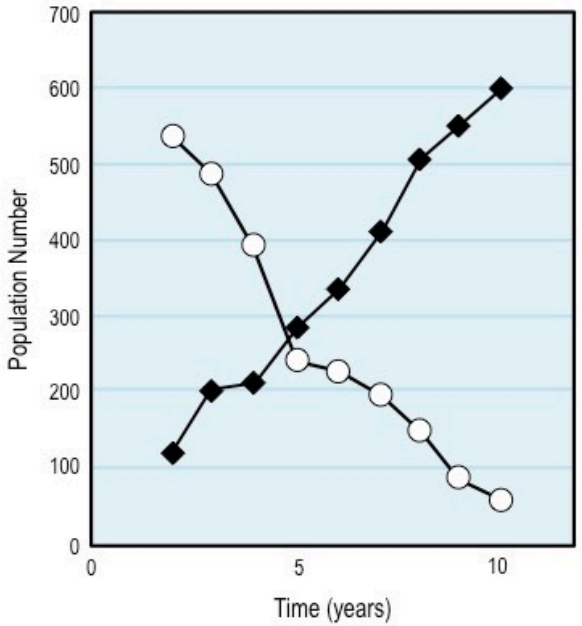

Post-Industrial Revolution

Avian vision models and field experiments determine the survival value of peppered moth camouflage

Olivia C. Walton[1] & Martin Stevens[1]

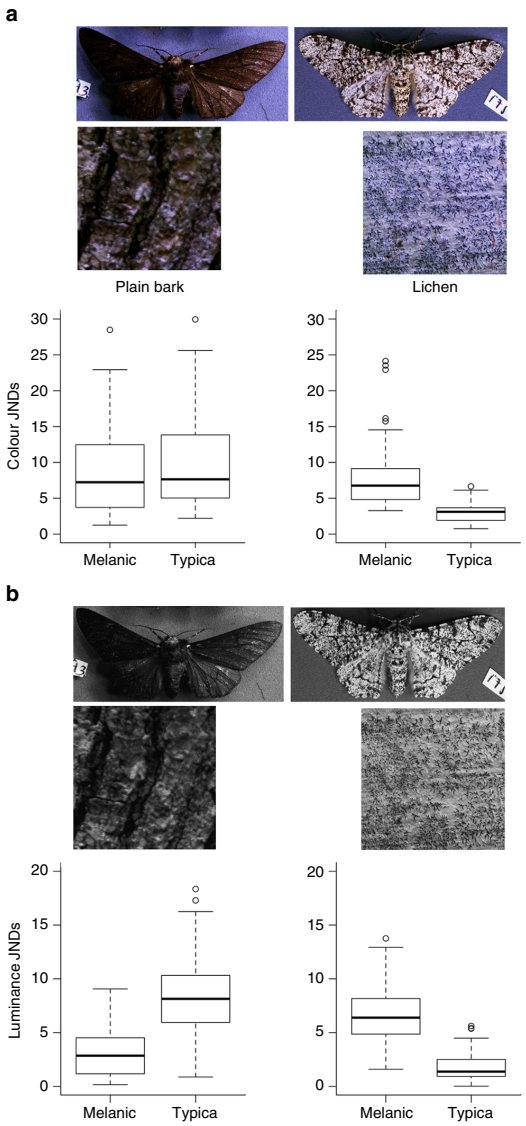

Fig. 1 Camouflage of peppered moth morphs to avian vision. Images show a melanic and a typical peppered moth morph to avian vision, along with samples of plain bark and lichen. **a** This set of images represent colour data ($n = 130$), comprised of cone response data for a longwave, mediumwave, shortwave, and UV cones (with UV and shortwave data combined into the blue image channel as images have only three layers). **b** This set of images represent data from avian double cones, showing luminance ($n = 130$). These images illustrate the better match for colour and luminance of *typica* compared to carbonaria against lichen backgrounds. Graphs are just noticeable difference (JND) results for colour (**a**) and luminance (**b**) of *typica* and *carbonaria* specimens against plain bark and lichen. JND data was statistically analysed using a general linear model, with colour data log-transformed. For colour (**a**) between the morphs, plain bark did not display significance ($p = 0.19$) whereas lichen bark did ($p = 6.66e^{-14}$). Both morphs displayed statistical significance for luminance (**b**); typica ($p < 2e^{-16}$) and melanic ($p < 2e^{-16}$). Boxplots display untransformed average JND values (bold line), the interquartile range (box component), range of minimum and maximum JND values (horizontal lines either end of range), and circle symbols signifying outlier results

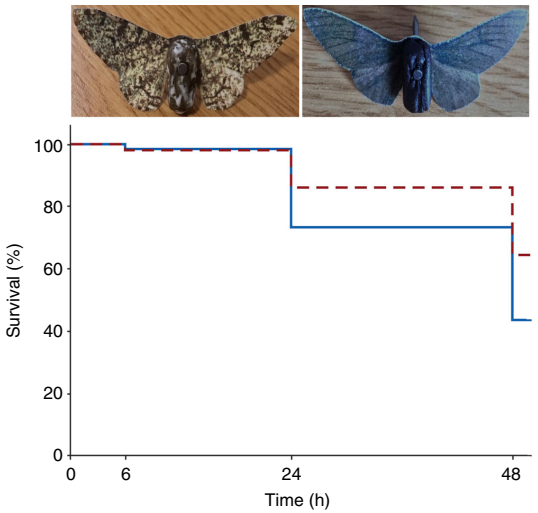

Fig. 2 Visualisation of the artificial predation experiment. Examples of the artificial moth targets made to match *typica* and *carbonaria* specimens show the components of the pastry body and the digitally colour calibrated paper wings. Statistical analysis was conducted to produce the non-parametric distribution plot of survival over time, using Kaplan–Meier estimation. Higher survival of targets matching *typica* moths than *carbonaria* moths were seen; graphically represented by the red dashed and solid blue lines, respectively ($n = 500$; $p < 2e^{-16}$)

Heredity

Heredity (2013) 110, 207–212

www.nature.com/hdy

REVIEW

The peppered moth and industrial melanism: evolution of a natural selection case study

LM Cook[1] and IJ Saccheri[2]

From the outset multiple causes have been suggested for changes in melanic gene frequency in the peppered moth *Biston betularia* and other industrial melanic moths. These have included higher intrinsic fitness of melanic forms and selective predation for camouflage. The possible existence and origin of heterozygote advantage has been debated. From the 1950s, as a result of experimental evidence, selective predation became the favoured explanation and is undoubtedly the major factor driving the frequency change. However, modelling and monitoring of declining melanic frequencies since the 1970s indicate either that migration rates are much higher than existing direct estimates suggested or else, or in addition, non-visual selection has a role. Recent molecular work on genetics has revealed that the melanic (*carbonaria*) allele had a single origin in Britain, and that the locus is orthologous to a major wing patterning locus in *Heliconius* butterflies. New methods of analysis should supply further information on the melanic system and on migration that will complete our understanding of this important example of rapid evolution.
Heredity (2013) **110,** 207–212; doi:10.1038/hdy.2012.92; published online 5 December 2012

Domestication/Artificial selection

The relations between evolution and domestication reconsidered - Implications for systematics, ecology, and nature conservation

Ulrich Zeller, Thomas Göttert*

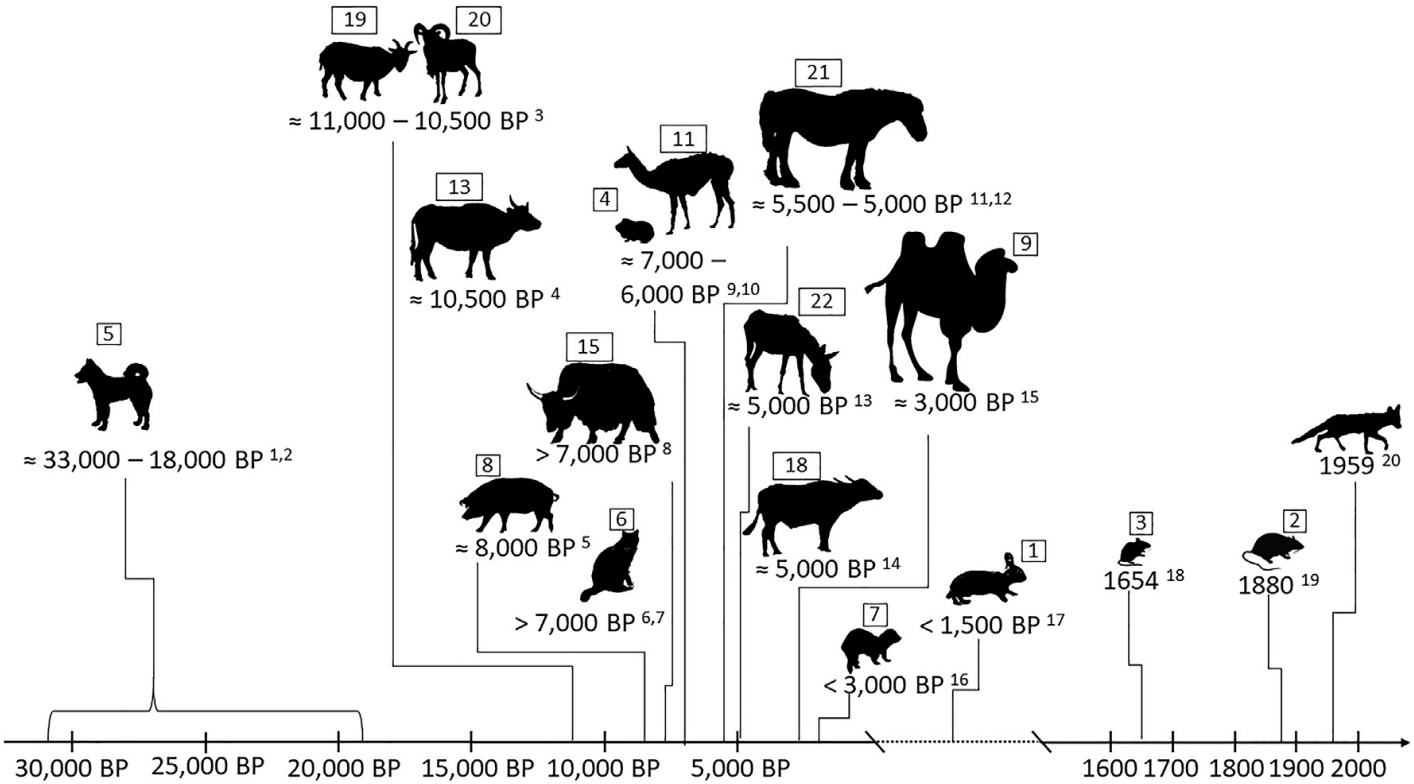

Fig. 3. Estimated starting points of domestication processes for different mammal species. Except for the red fox *(Vulpes vulpes)* these examples are also referred to in Table 1. Digits in boxes refer to sequential numbers of domesticated forms in Table 1. Superscript digits refer to references with temporal classification: 1) Druzhkova et al. (2013); 2) Thalmann et al. (2013); 3) Zeder, 2008; 4) Helmer et al. (2005); 5) Albarella et al. (2006); 6) Driscoll et al. (2007); 7) Ottoni et al. (2017), 8) Qiu et al. (2015), 9) Sandweiss and Wing (1997); 10) Kadwell et al. (2001); 11) Warmuth et al. (2012); 12) Gaunitz et al. (2018); 13) Rossel et al. (2008); 14) Kierstein et al. (2004); 15) Potts (2004); 16) Thomson (1951); 17) Carneiro et al. (2011); 18) Tokuda, 1935; 19) Castle (1947); and 20) Trut (1999).

ORIGINS AND PRIMARY REGIONS OF DIVERSITY OF AGRICULTURAL CROPS

Khoury CK, Achicanoy HA, Bjorkman AD, Navarro-Racines C, Guarino L, Flores-Palacios X, Engels JMM, Wiersema JH, Dempewolf H, Sotelo S, Ramirez-Villegas J, Castañeda-Álvarez NP, Fowler C, Jarvis A, Rieseberg LH, and Struik PC (2016). Origins of food crops connect countries worldwide. Proc. R. Soc. B 283: 20160792. DOI: 10.1098/rspb.2016.0792.

CIAT
International Center for Tropical Agriculture
Since 1967 Science to cultivate change

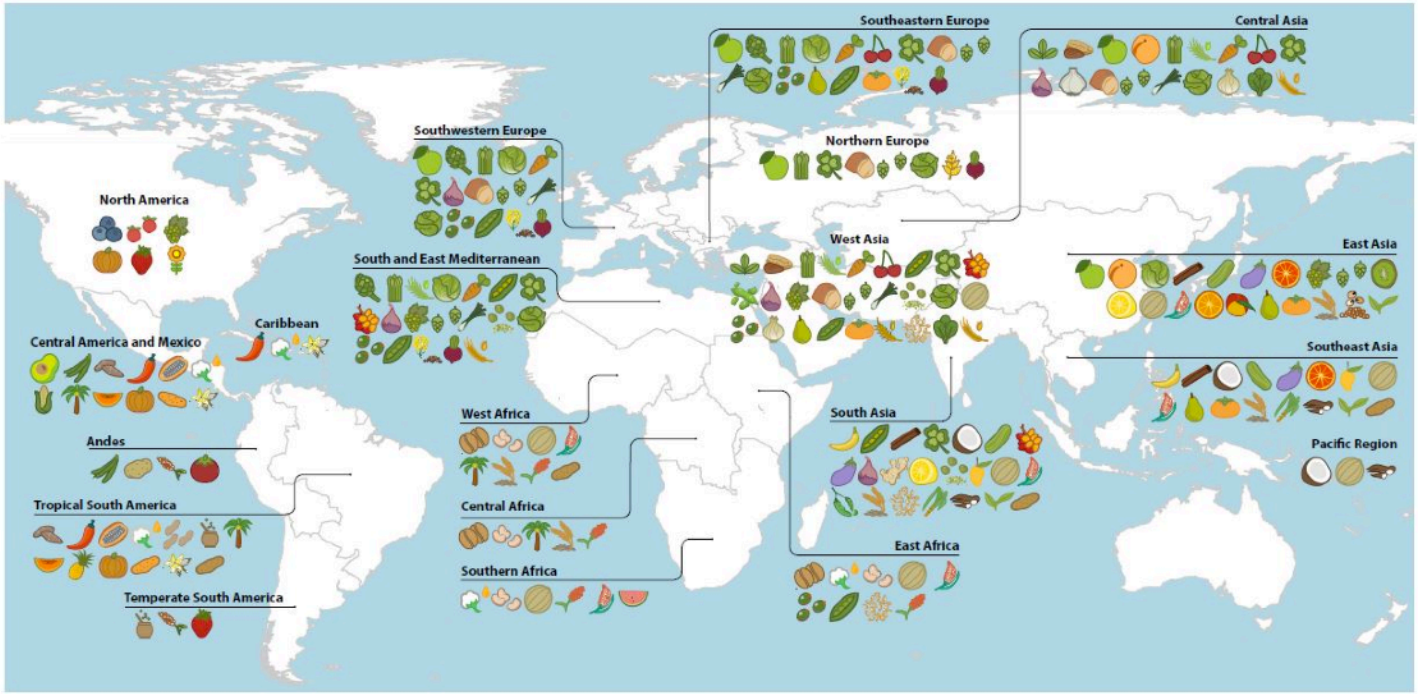

Alfalfa, Almonds, Apples, Apricots, Artichokes, Asparagus, Avocados, Bananas & plantains, Barley, Beans, Blueberries, Cabbages, Carrots, Cassava, Cherries, Chickpeas, Chillies & peppers, Cinnamon, Clover, Cocoa beans, Coconuts, Coffee, Cottonseed oil, Cowpeas, Cranberries, Cucumbers, Dates, Eggplants, Faba beans, Figs, Garlic, Ginger, Grapefruit, Grapes, Groundnut, Hazelnuts, Hops, Kiwi, Leeks, Lemons & limes, Lentils, Lettuce, Maize, Mangoes, Mate, Melons, Millets, Oats, Olives, Onions, Oranges, Palm oil, Papayas, Peaches & nectarines, Pears, Peas, Pigeonpeas, Pineapples, Plums, Potatoes, Pumpkins, Quinoa, Rape & mustard seed, Rice, Rye, Sesame, Sorghum, Soybean, Spinach, Strawberries, Sugar beet, Sugarcane, Sunflower, Sweet potatoes, Taro, Tea, Tomatoes, Vanilla, Watermelons, Wheat, Yams


Small Dog Breeds
101DogBreeds
Chihuahua
Maltese
Pug
Japanese Terrier
Papillon
Coton de Tulear
Pekingese
Pomeranian
Biewer Terrier
Bedlington Terrier
Yorkshire Terrier
Lowchen
Brussels Griffon
Miniature Pinscher
Teddy Roosevelt Terrier
Havanese
Affenpinscher
Miniature Schnauzer
Lhasa Apso
Bichon Frise
Boston Terrier
Lancashire Heeler
Shih Tzu
American Eskimo Dog
Border Terrier
Shiba Inu
Cavalier King Charles Spaniel
Dandie Dinmont Terrier
Jack Russell Terrier
Silky Terrier
Medium Dog Breeds
101DogBreeds
Bearded Collie
Border Collie
Canaan Dog
Treeing Tennessee Brindle
Australian Cattle Dog
Bulldog
Norwegian Elkhound
Bohemian Shepherd
Carolina Dog
Brittany
Pharaoh Hound
Keeshond
Nova Scotia Duck Tolling Retriever
English Springer Spaniel
Standard Schnauzer
Australian Stumpy Tail Cattle Dog
Welsh Springer Spaniel
Karelian Bear Dog
Spanish Water Dog
Croatian Sheepdog
Jindo
Polish Lowland Sheepdog
American Water Spaniel
Australian Kelpie
German Pinscher
Boykin Spaniel
Soft Coated Wheaten Terrier
Mudi
Whippet


Big Dog Breeds
101DogBreeds
English Mastiff
Caucasian Shepherd
Saint Bernard
Tibetan Mastiff
Bloodhound
Boerboel
Great Pyrenees
Neapolitan Mastiff
Broholmer
Newfoundland Dog
Afghan Hound
Akita
Irish Setter
Dogue de Bordeaux
Borzoi
Kuvasz
Akita
Bernese Mountain Dog
Cane Corso
Irish WolfHound
Golden Retriever
Boxer
Otterhound
Scottish Deerhound
Great Dane
Beauceron
German Shepherd
Rhodesian Ridgeback
Poodle
Curly-Coated Retriever
Leonberger
Doberman
Saluki
Hovawart
Dalmatian
Vizsla
Chow Chow

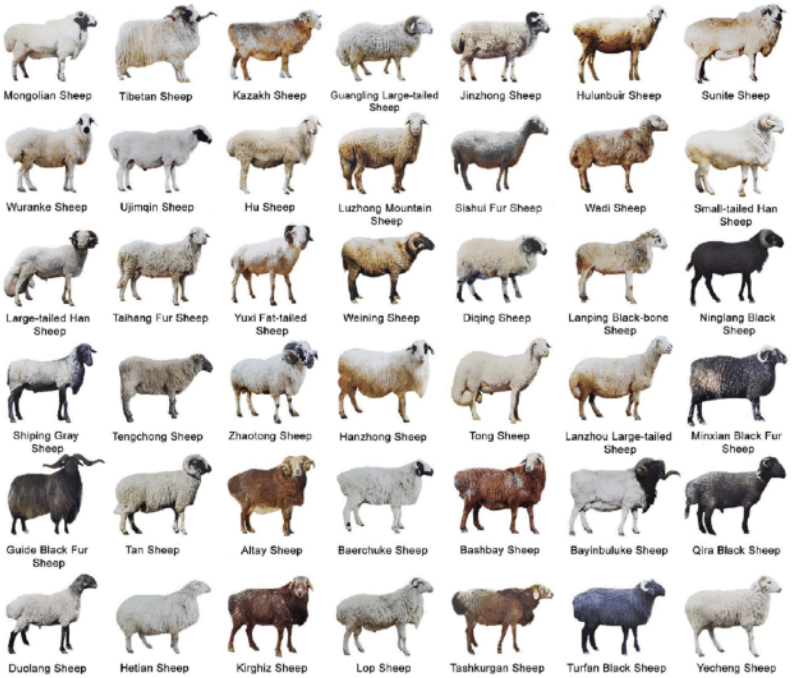

Updated 8-12-2020


Benihoppe
Kaorino
Hatsukoi no Kaori
White Goblin
Santa Red
Shanghai Sweet-Beauty
Shanghai Angel
Snow White
Little white
Yue Xin
Yue Xiu

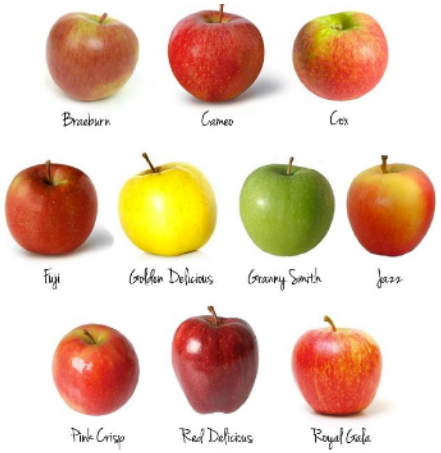
Braeburn
Cameo
Cox
Fuji
Golden Delicious
Granny Smith
Jazz
Pink Crisp
Red Delicious
Royal Gala


Hard Red Winter
Hard Red Spring
Soft Red Winter
Soft White
Hard White
Durum


Thoory
Samany
Saidi
Premium Medjool
Pitted Deglet Noor
Large Medjool
Kway
Khalasa
Khaisab
Khadrawy
Jumbo Medjool
Honey
Halawy
Deglet Noor Whole
Dayri
Black McGill
Black Laflin
Black Beauty
Black 8 Ball
Barhi
Abbada
Zahidi

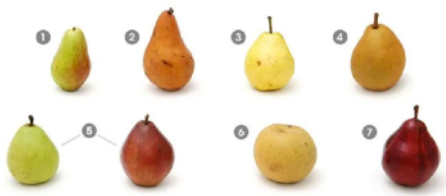

Disclaimer

Figures, photos, and graphs in my lectures are collected using google searches. I do not claim to have personally produced the material (except for some). I do cite only articles or books used. I thank all owners of the visual aid that I use and apologize for not citing each individual item. If anybody finds the inclusion of their material in my lectures a violation of their copy rights, please contact me via email.

hhalhaddad@gmail.com